

Cleanup of Oil Zones After a Gel Treatment

R.S. Seright, SPE, New Mexico Petroleum Recovery Research Center

Summary

A simple mobility-ratio model was used to predict cleanup times for both fractured and unfractured production wells after a gel treatment. The time to restore productivity to a gel-treated oil zone (1) was similar for radial vs. linear flow, (2) varied approximately with the cube of distance of gel penetration, (3) varied inversely with pressure drawdown, (4) varied inversely with the k_w at S_{or} in the gel-treated region, and (5) was not sensitive to the final k_o at S_{wr} . Although k_o at S_{wr} (after gel placement) had no effect on the cleanup time, it strongly affected how much of the original oil productivity was ultimately regained.

Introduction

Utility of Disproportionate Permeability Reduction. In mature reservoirs, wells typically produce more water than hydrocarbon. In many wells, hydrocarbon productivity could be increased significantly if the water production rate could be reduced. For these cases, the water and hydrocarbon must flow to the wellbore through different pathways (i.e., some zones have high fractional hydrocarbon flow, while other zones have high fractional water flow) (Liang et al. 1993). Because of physical or economic constraints, remedial chemical treatments (e.g., gel treatments) that are intended to plug water strata are often placed without zone isolation. Consequently, the injected fluids and chemicals penetrate into both hydrocarbon and water zones, and the operator must be concerned about damage to hydrocarbon productivity (Liang et al. 1993; Seright 1988). Certain water-based gels and water-soluble polymers (after adsorption or entrapment in rock) can reduce permeability to water much more than that to hydrocarbon (Seright et al. 2006; Zaitoun and Kohler 1988). Basic engineering calculations reveal that materials that provide “relative permeability modification” or “disproportionate permeability reduction” are currently of far more practical use when treating linear flow features (e.g., fractures) than when treating radial matrix flow problems (e.g., wells without fractures) (Seright website; Seright et al. 1998; Marin et al. 2002). For these materials to effectively treat radial matrix flow, they should reduce permeability to water by more than a factor of 10 (and preferably by more than a factor of 20). At the same time, they must reduce permeability to oil by less than a factor of two if oil zones are not protected during placement (Seright website). In contrast, when treating fractures, a significant oil residual resistance factor (permeability reduction value for oil) can be tolerated so long as (1) the permeability to water is reduced much more (e.g., >50 times more) than that to oil and (2) the distances of gelant leakoff from the fracture faces are controlled (Seright website; Seright et al. 1998; Marin et al. 2002).

Cleanup Behavior. For many field applications in production wells, oil productivity gradually increased or “cleaned up” during the first weeks after gel treatments were applied (Marin et al. 2002; Lane and Sanders 1995; Stanley et al. 1996). To understand this phenomenon, we studied the dependence of oil and water permeabilities on throughput during various cycles of oil and water injection after gel or polymer placement in laboratory cores.

Behavior of a Cr(III)-Acetate-HPAM Gel

In our experiments, the gel contained 0.5% Ciba Alcoflood 935™ HPAM, 0.0417% Cr(III) acetate, 1% NaCl, and 0.1% CaCl₂ at 27°C. The hydrolyzed polyacrylamide polymer (HPAM) had a molecular weight of approximately 5×10⁶ daltons and a degree of hydrolysis of 5 to 10%. The first Berea sandstone core used was 7.8 cm long and 3.8 cm in diameter, with an absolute permeability of 746 md and porosity of 0.21. All flooding steps were performed using a fixed pressure gradient of 40 psi/ft. Prior to gel injection, the core was flooded (with 3.34-cp hexadecane) to residual water saturation ($S_{wr}=0.43$), where an endpoint permeability to oil (k_o) of 508 md was observed. (In this paper, our endpoint permeabilities are effective permeabilities at residual saturations. They are not relative permeabilities.) Next, the core was flooded (with 0.93-cp brine) to residual oil saturation ($S_{or}=0.37$), where an endpoint permeability to water (k_w) of 120 md was measured. Then, 6 pore volumes (PV) of Cr(III)-acetate-HPAM gelant were injected, and the core was shut in for 4 days to allow gelation. After gelation, hexadecane was injected using a fixed pressure gradient of 40 psi/ft. The solid circles in Fig. 1 demonstrate that permeability to oil increased gradually from 2 to 105 md during the course of 100 PV. The open circles in Fig. 1 show the permeability when water was injected after the previously described oil-injection stage. In contrast to the oil behavior, permeability to water stabilized at 0.17 md within a few tenths of 1 PV. During the second and third cycles of oil injection (solid triangles and squares in Fig. 1), permeability again gradually increased over the course of 100 PV. The permeability to oil followed the same trend for all three cycles (although the final permeability was 60% greater for the second and third cycles than for the first cycle). During the second cycle of water injection (open triangles in Fig. 1), the permeability stabilized at 1.1 md within 1 PV.

Mobility Ratios

The concept of mobility ratio can explain the behavior in Fig. 1. Here, mobility, k/μ , is defined as the effective permeability of a porous material to a given phase divided by the viscosity of that phase. Mobility ratio, M , is defined as mobility of the displacing phase divided by the mobility of the displaced phase. Consider a case in which water is injected into an oil zone to displace oil away from a well (Fig. 2), where oil and water viscosities and endpoint permeabilities are given in the previous section. As injected water displaces oil away from the wellbore, the “endpoint” mobility ratio is

$$M = (k_w/\mu_w)/(k_o/\mu_o) = (120/0.93)/(508/3.34) = 0.85. \dots (1)$$

Because $M < 1$, the displacement is stable, and a fairly sharp “shock front” separates the mobile oil and water phases.

Next, consider the mobility ratio when the well is returned to production, and oil displaces water toward the well:

$$M = (k_o/\mu_o)/(k_w/\mu_w) = (508/3.34)/(120/0.93) = 1.2. \dots (2)$$

In this case, the mobility ratio is slightly greater than one, and therefore is slightly unfavorable. However, the value is close enough to unity that the displacement is nearly piston-like.

Now, consider the case when a polymer solution or gelant is injected to displace either oil or water away from a production well (Fig. 3). If the displacement is stable or near-stable before polymer or gelant injection, it is also stable during injection of polymer solutions or gelant, because these fluids are usually more viscous

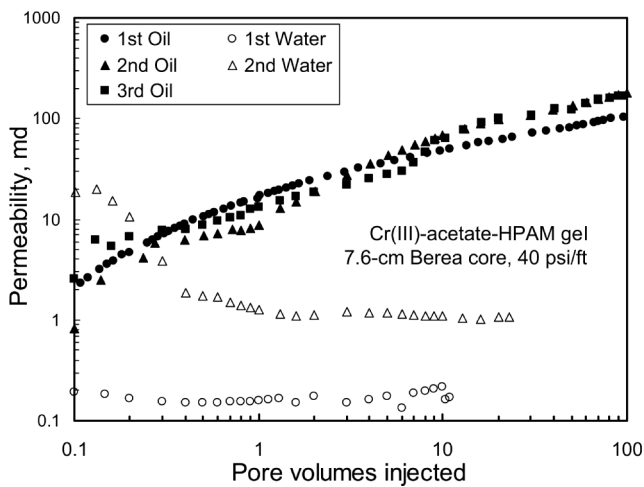


Fig. 1—Permeability to oil and water after gel placement in a Berea core.

than water. (The notable exception occurs when the oil has a high viscosity.)

After placement of the polymer solution or gelant and after gel formation, what happens when a well is returned to production? In the oil zone, oil with a relatively high mobility attempts to flow through gel that is basically immobile. Water can flow within the gel, although the permeability is very low (Seright 1993). Therefore, a mobility ratio can be estimated. For example, if $k_o = 508$ md at S_{wr} , $\mu_o = 3.34$ cp, $k_w = 0.17$ md in the gel treated region, and $\mu_w = 0.93$ cp, then the mobility ratio is $(508/3.34)/(0.17/0.93) = 830$. With this highly unfavorable mobility ratio, the displacement is very inefficient, and oil forms wormholes through the gel-treated region (Fig. 4). For inefficient displacements, many PV of throughput are required to achieve stabilization (Seright 1991; Koval 1963)—just as observed during oil injection after gel placement (Fig. 1). Concerning the formation of oil wormholes in the gel-treated region, recognize that the oil cannot actually enter or flow through the gel polymeric structure. As oil pushes on the gel, water flows through the gel structure and exits the gel-treated region at the wellbore. The pressure exerted by the oil on the gel causes some dehydration and the start of an oil pathway through the gel (Krishnan et al. 2000). As illustrated in Fig. 4, this pathway becomes accentuated with time, resulting in a wormhole pattern.

Finally, consider the case in which a water zone is returned to production after gel placement (Fig. 5). On first consideration, we expect an unfavorable mobility ratio and an inefficient displacement similar to that illustrated in Fig. 4. After all, water outside the gel-treated region is much more mobile than water inside the gel-treated region. However, in contrast to the oil, water can actually enter and flow through the gel structure. Upon entry, this water immediately becomes part of the gel. No gel dehydration occurs, no wormhole pathways form, and the displacement remains stable. The gel remains in exactly the same location, but water just flows through the gel, experiencing a very low permeability. Therefore, the effective permeability to water stabilizes rapidly, as observed in Fig. 1.

In summary, the concepts of mobility ratio and stable vs. unstable displacement explain the behavior in Fig. 1.



Fig. 3—Mobility ratios are usually favorable (stable displacement) during injection of gelant or polymer solutions.

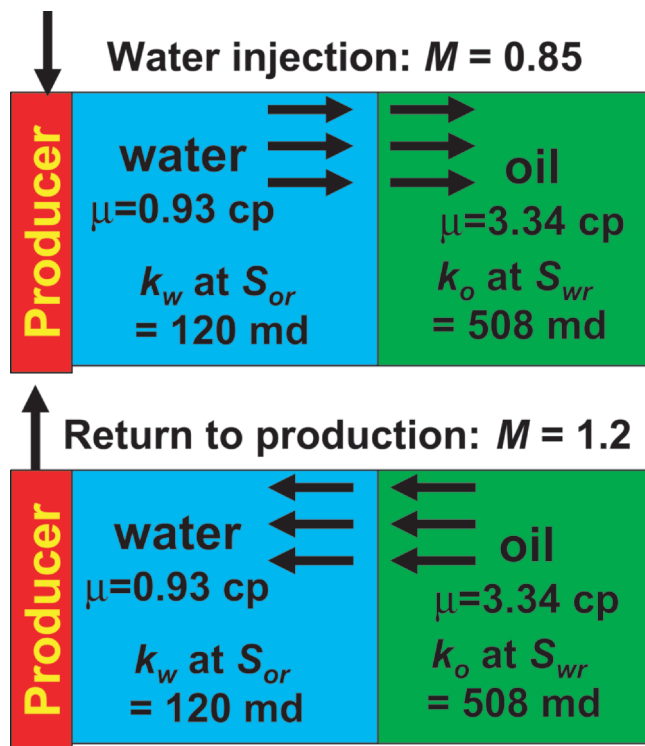


Fig. 2—Stable displacements during water injection, followed by return to production (before gel placement).

Permeability to Water During Many Experiments

Table 1 lists stabilized final permeability to water after gel placement for many experiments. Three porous media were examined, including strongly water-wet Berea sandstone and fused silica and strongly oil-wet porous polyethylene. Initial core permeabilities ranged from 738 to 15,270 md. Most cores were ~7.6 cm long, although two Berea cores were 15.2 cm long. At S_{or} before gel placement, typical relative permeabilities to water were 0.16 in Berea sandstone, 0.5 in porous polyethylene, and 0.27 for fused silica. The pressure gradient applied ranged from 10 to 100 psi/ft. The k_w values were measured under several different conditions, including (1) when water was the first fluid injected after gel placement, (2) when oil was the first fluid injected after gel placement and then followed by water injection, and (3) when at least one cycle of water and oil were injected before the k_w measurement.

For cases in Table 1, permeability to water stabilized at the reported value within 1 PV and remained stable for up to 100 PV. For five cases in which water was the first fluid injected after gel placement, permeability to water averaged 0.26 md. This value was of the order expected if all aqueous pore space was filled with gel and water only flowed through the gel (Seright 1993).

For several cases flooded at 100 psi/ft (end of Table 1), k_w values were high (up to 211 md), suggesting significant gel breakdown at this high-pressure gradient.

For cases in which at least one cycle of oil preceded the k_w measurement, permeability ranged from 0.17 to 211 md, but was commonly between 1 and 3 md.

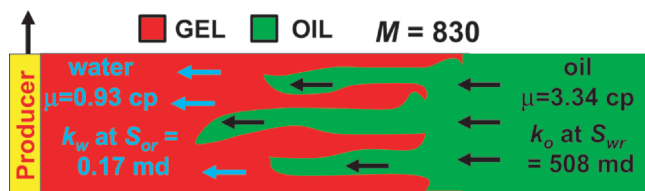


Fig. 4—Unfavorable mobility ratio when an oil zone is returned to production after gel placement.

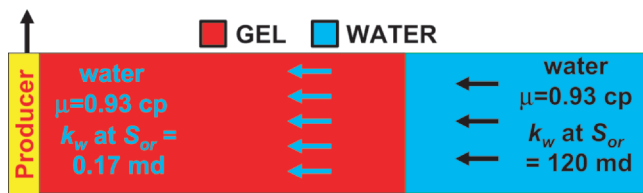


Fig. 5—Stable displacement when a water zone is returned to production after gel placement. $M=706$, but displacement is still stable because the entering water becomes part of the gel.

An experiment was performed to test how persistently the gel would reduce permeability during continuous water flow. A porous polyethylene core (6.4 cm long, 3.8 cm in diameter) was saturated with our standard Cr(III)-acetate-HPAM gel [0.5% Alcoflood 935, 0.0417% Cr(III) acetate, 1% NaCl, 0.1%CaCl₂]. After gelation, brine (1% NaCl, 0.1%CaCl₂) was allowed to flow through the gel-filled core using a constant pressure gradient of 30 psi/ft. This pressure gradient was established by placing a 442-cm-high column of brine over the core. Fig. 6 shows the results. Over the course of 500 days, the permeability to water remained fixed at approximately 60 μ d.

Permeability to Oil During Many Experiments

In contrast to the behavior during water injection, the apparent permeability steadily increased during injection of 100 PV of oil. Fig. 7 shows overall core k vs. PV during oil injection for many experiments (performed with those in Table 1). The observed trends matched expectations for an unstable displacement. Conventional relative permeability equations (Lake 1989) can be readily used to model this behavior (e.g., see Appendix A of

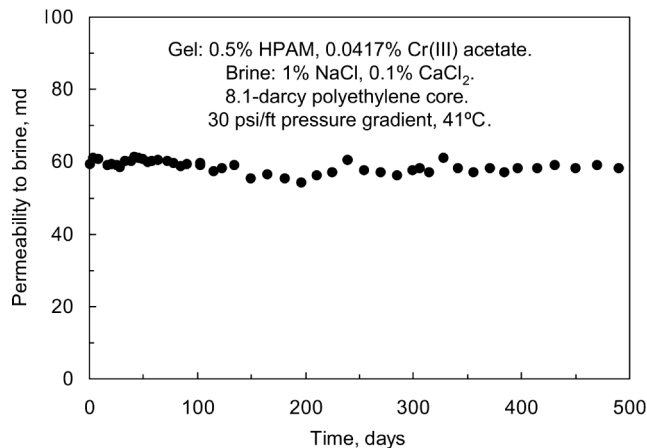


Fig. 6—Permeability to brine vs. time.

Seright 2004). (For modeling in this paper, the water and oil saturation exponents, n_w and n_o , were 1 or 2.)

$$k_{rw} = k_{rw}^o [(S_w - S_{wr}) / (1 - S_{or} - S_{wr})]^{n_w} \dots \dots \dots (3)$$

$$k_{ro} = k_{ro}^o [(1 - S_{or} - S_w) / (1 - S_{or} - S_{wr})]^{n_o} \dots \dots \dots (4)$$

The thin solid curve in Fig. 7 shows predictions when 3-cp oil (with endpoint $k_o = 100$ md) was injected into a core (at S_{or} after gel placement) where 1-cp water had an endpoint $k_w = 0.26$ md. For the thick solid curve, endpoints $k_o = 1,000$ md and $k_w = 1$ md. (In both cases, $S_{or} = 0.368$ and $S_{wr} = 0.432$.) The two curves provide lower and upper limits of behavior for the Cr(III)-acetate-

TABLE 1— k_w VALUES AFTER GEL PLACEMENT					
Core	Core Length (cm)	Initial Core (k, md)	dp/dl (psi/ft)	Condition	k_w at S_{or} After Gel (md)
Berea	7.8	746	40	water after oil	0.17
Berea	7.8	746	40	2nd water after oil	1.11
Berea	15.2	738	40	water after oil	1.93
Berea	15.2	738	40	2nd water after oil	2.25
PE	7.6	8,400	10	water after oil	1.56
PE	7.6	10,000	30	water after oil	1.49
PE	7.6	7,410	100	water after oil	2.83
PE	7.6	13,550	10	water after oil	21.3
PE	7.6	8,530	30	water after oil	2.63
PE	7.6	5,440	100	water after oil	0.63
PE	7.6	15,270	10	water 1st	0.37
PE	7.6	9,530	30	water 1st	0.24
PE	7.6	9,530	30	2nd water after oil	1.17
PE	7.6	6,204	100	water 1st	0.32
PE	7.6	6,204	100	2nd water after oil	0.74
Silica	7.6	2,390	10	water 1st	0.12
Silica	7.6	2,390	10	2 nd water	0.35
Silica	7.6	1,820	30	water 1st	0.23
Silica	7.6	1,820	30	2nd water	0.22
Silica	7.6	1,970	10	water after oil	0.45
Silica	7.6	2,110	30	water after oil	3.1
Silica	7.6	1,330	100	water after oil	13.6
Silica	7.6	1,330	100	2nd water after oil	211
Silica	7.6	850	100	water 1st	131

Average k_w for five "water first" cases: 0.26 md (\pm 0.1 md)
(Excluding 100-psi case in silica); PE = polyethylene

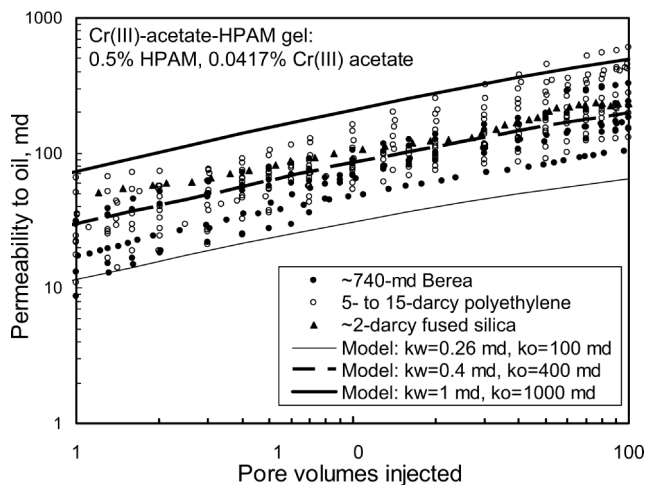


Fig. 7— k_o after gel placement for many experiments.

HPAM gel. The dashed curve provides an intermediate case where endpoints $k_o = 400$ md and $k_w = 0.4$ md.

In these experiments, the lowest pressure gradient used was 10 psi/ft. We wondered whether a minimum pressure gradient existed, below which oil would not penetrate through the gel. After placement of Cr(III)-acetate-HPAM gel in a 8-darcy polyethylene core, oil was used to apply pressure gradients of 0.43 psi/ft for 6 days, followed by 0.86 psi/ft for 10 days, and 1.3 psi/ft for 15 days. No flow was detected (i.e., $k_o < 1 \mu\text{d}$). Oil flow was finally observed after the pressure gradient was raised to 1.7 psi/ft. Therefore, in this polyethylene core, the minimum pressure gradient needed to initiate oil flow was between 1.3 and 1.7 psi/ft. For field applications where flow is radial around the wellbore (i.e., unfractured wells), pressure gradients are quite high near the wellbore and low deep in the reservoir. Pressure gradients around 1.7 psi/ft are typically present between 50 and 100 ft from a flowing well (depending, of course, on the production rate, fluid viscosity, and formation permeability). These observations raise additional concern for large volume gelant treatments that may penetrate too far into porous rock.

Predicting Oil-Zone Cleanup for Field Applications

How quickly will oil productivity increase after a gel treatment where gelant invaded the oil productive zones? This question can readily be answered using a simple mobility ratio model, where the key input parameters are endpoint k_w and k_o . Appendices B and C of Seright (2004) list the model code for the predictions presented in this section. In these examples, the external drainage distance or

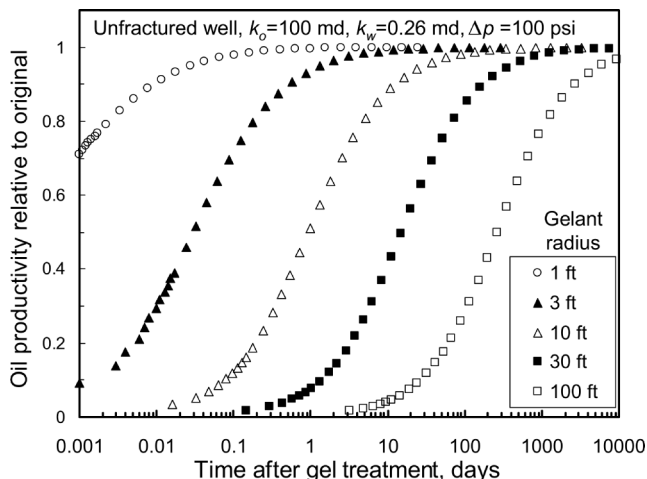


Fig. 9—Effect of radius of gel penetration in an unfractured well.

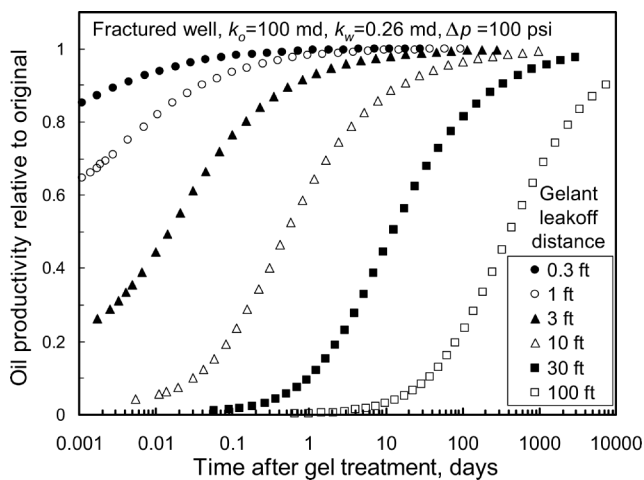


Fig. 8—Effect of distance of gel penetration from a fracture face.

radius was 500 ft, $S_{or} = 0.368$, and $S_{wr} = 0.432$. For radial cases, the wellbore radius was 0.5 ft. The first predictions assumed that the oil residual resistance factor (F_{rro}) in the gel-treated region approached unity after a large volume of oil throughput (i.e., k_o at S_{wr} was the same in gel-treated and untreated rock). In the following figures, time (during flow) is plotted on the x -axis, while the y -axis plots oil productivity (i.e., the oil productivity index) relative to the oil productivity if no gel treatment had been applied.

Effect of Distance of Gelant Penetration. Figs. 8 and 9 show the influence of distance of gelant penetration on the recovery time for oil productivity for fractured (linear flow) and unfractured (radial flow) production wells. Pressure drawdown (Δp , between the external drainage distance and the wellbore) was fixed at 100 psi. As expected, the time for oil cleanup increased significantly with increased distance of gel penetration. For both fractured and unfractured cases, gelant penetration distances less than 10 ft provided the most desirable times to recover oil productivity (i.e., a day or less). Caution: for large distances of gelant penetration, the pressure gradient may be too low (e.g., < 1.7 psi/ft) to allow oil to initiate flow through the gel (see the previous section).

Based on Figs. 8 and 9, Fig. 10 was prepared, showing the time for a well to regain 10, 50, and 90% of its original oil productivity. Recovery times were similar for linear and radial flow. Cleanup time (t) varied approximately with the cube of gel penetration (L_p). The solid curve and triangle symbols illustrate this point for regaining 50% productivity. The circles indicate the time to regain 10% of the original productivity, while the squares show time to recover 90% of the original productivity.

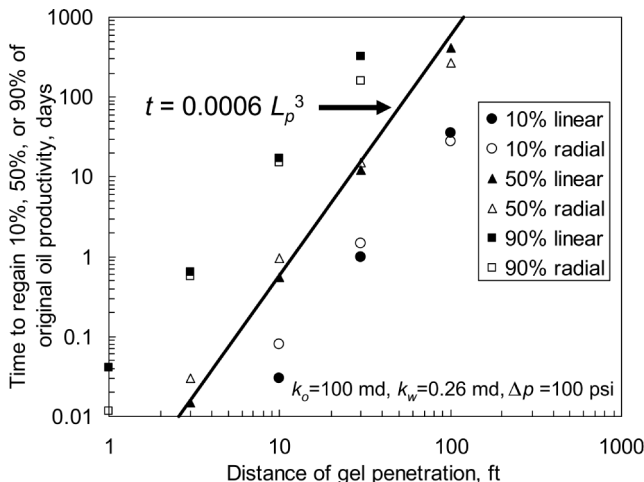


Fig. 10—Cleanup time in linear vs. radial flow.

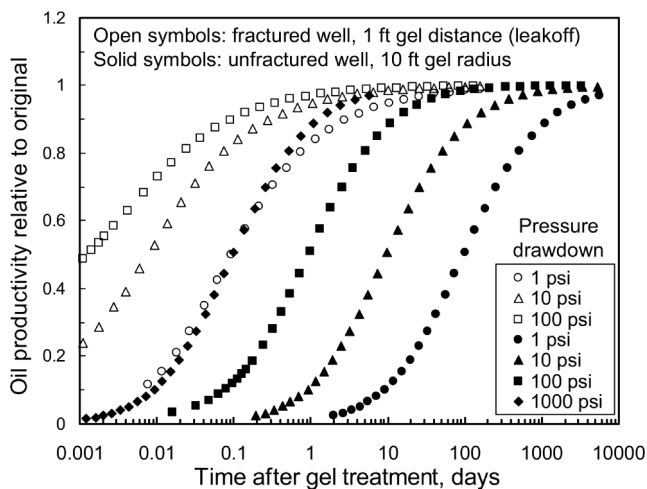


Fig. 11—Effect of pressure drawdown on oil-zone cleanup.

Alternatively, the oil production rate (q) at any time can be estimated using Eq. 5, where q_{final} is the ultimate post-treatment oil production rate, t is time in days, Δp is pressure drawdown in psi, k_w is permeability in md, and L_p is distance or radius of gelant penetration in ft. A spreadsheet that performs this calculation (and others) is available at the website <http://baervan.nmt.edu/randy/>. Eq. 5 worked best for relatively small distances of gelant penetration.

$$q = q_{\text{final}}(2/\pi) \arctan[(64 t \Delta p k_w/L_p^3)^{\pi/4}]. \quad (5)$$

An updated method for predicting clean up times can be found in Seright (2006).

Effect of Pressure Drawdown. The time for cleanup of an oil zone varied inversely with pressure drawdown. Increasing the pressure drawdown from 1 to 1,000 psi decreased the cleanup time 1,000-fold (solid symbols in Fig. 11). For unfractured wells where the radius of gelant penetration was 10 ft, relatively high-pressure drawdowns were needed to clean up the oil zones in a reasonable time period. For gel treatments in fractured production wells where the distance of gelant leakoff from fracture faces was relatively small, oil zones cleaned up quickly even for low drawdowns (open symbols in Fig. 11).

Effect of k_w and k_o . The time for cleanup of an oil zone varied inversely with the endpoint k_w after gel formation, but was not sensitive to the endpoint k_o (Fig. 12). Cleanup time decreased by a factor of 100 as k_w increased from 0.1 to 10 md (when k_o was held constant at 1,000 md). In contrast, when k_w was held constant at 0.26 md, the cleanup time was basically unaffected as k_o increased from 100 to 10,000 md.

Note that the open and solid triangles in Fig. 12 show predictions associated with lower and upper limits that bracket the data in Fig. 7. These data suggest a maximum four-fold variation in cleanup time for the experiments in Fig. 7.

Summary. In this analysis, the time to restore productivity to a gel-treated oil zone was

- Similar for radial and linear flow.
- Approximately proportional to the cube of distance of gel penetration.
- Inversely proportional to pressure drawdown.
- Inversely proportional to the endpoint k_w at S_{wr} in the gel-treated region.
- Not sensitive to the endpoint k_o at S_{wr} .

Effect on Ultimate Oil Productivity

Although k_o at S_{wr} (after gel placement) has no effect on the cleanup time (Fig. 12), it does impact how much of the original oil productivity can ultimately be regained after a gel treatment. In the

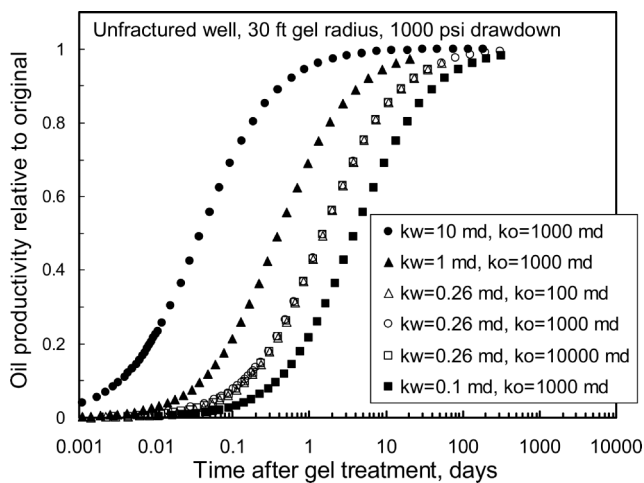


Fig. 12—Effect of k_w and k_o on oil-zone cleanup.

previous analysis, we assumed that the permeability to oil in the gel-treated region would eventually approach k_o at S_{wr} in the untreated region. What happens if permeability to oil in the gel-treated region cannot rise to match the original k_o ?

Productivity reduction from a gel treatment is described by Eq. 6 for linear flow and by Eq. 7 for radial flow (Seright 1988):

$$q/q_o = L_e / [(F_{rr} - 1)L_p + L_e] \quad (6)$$

and

$$q/q_o = \ln(r_e/r_w) / [(F_{rr} \ln(r_p/r_w) + \ln(r_e/r_w))]. \quad (7)$$

In these equations, q/q_o is the ultimate productivity relative to productivity before the gel treatment, r_e is the external drainage radius, L_e is the external drainage distance, and r_w is the wellbore radius. In our examples, $L_e = r_e = 500$ ft and $r_w = 0.5$ ft. F_{rr} is the ultimate or stabilized residual resistance factor (i.e., the factor by which the permeability to oil or water is reduced by the gel). Figs. 13 and 14 show results of ultimate productivity calculations for linear and radial flow. These figures are applicable to either oil or water flow.

Gel Penetration From Fracture Faces. Fig. 15 simplifies Fig. 13 by plotting $(F_{rr} - 1)L_p$ on the x-axis. To maintain high oil productivity in a fractured well, the x-axis parameter should be less than 100 ft (and preferably less than 40 ft). To maintain low water productivity, the x-axis parameter should be greater than 3,000 ft. These objectives can be achieved by controlling F_{rr} or the distance of gel penetration (L_p) or both.

What range of oil residual resistance factors (F_{rro}) occurred with the Cr(III)-acetate-HPAM gel? In Berea, k_o at S_{wr} before gel placement typically was approximately 500 md (Fig. 1). Given the lower-limit curve in Fig. 7, the lower limit of k_o at S_{wr} after gel placement (after many PV of oil throughput) was 100 md. For this case, $F_{rro} = 5$ (500/100). From Fig. 15, a high ultimate oil productivity would be retained [i.e., $(F_{rr} - 1)L_p < 40$ ft] if the distance of gel penetration was less than 10 ft [i.e., $40/(5-1)$]. For some experiments (Fig. 7), the permeability to oil in Berea (after gel) exceeded 300 md and the ultimate permeability approached k_o at S_{wr} for the untreated rock. In these cases, $F_{rro} < 2$, and the maximum acceptable distance of gel penetration (from the fracture faces) could be 40 ft or more.

Higher oil-resistance factors and lower acceptable distances of gel penetration were noted for the polyethylene and fused silica cores. In polyethylene, k_o at S_{wr} typically was between 5 and 10 darcys before gel placement, depending on the initial (absolute) permeability of the core. Given these values and the k_o values from Fig. 7, F_{rro} values could range from 5 to 77 (i.e., 5,000/1,000 to 10,000/130). If $F_{rro} = 77$, the maximum allowable gel penetration (from Fig. 15) is 0.5 ft [i.e., $40/(77-1)$].

A similar analysis can be performed for the fused silica data. Here, k_o at S_{wr} was typically about 1,000 md before gel placement.

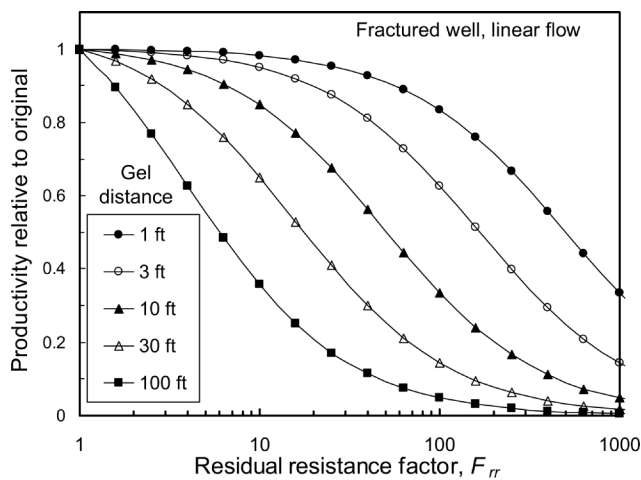


Fig. 13—Ultimate productivity after gel placement in a fractured production well.

Ultimate F_{rr} values could range from 2 to 5, and a conservative maximum allowable gel penetration would be 10 ft from the fracture faces [i.e., $40/(5-1)$]. Our analysis in the previous section (open triangles in Fig. 8) indicated that restoration of oil productivity should occur fairly quickly if gel penetration is less than 10 ft.

The previous analysis focused on gel penetration into an oil zone. Of course, in addition to minimizing damage to oil productivity, a gel treatment should substantially reduce water productivity (Seright website; Seright et al. 1998; Marin et al. 2002). As mentioned, the parameter, $(F_{rr} - 1)L_p$, should be greater than 3,000 ft in the water zone. To assess the appropriate distances of gel penetration, the water residual resistance factor, F_{rrw} , is needed. In turn, determining F_{rrw} requires knowledge of k_w at S_{or} before and after gel placement. Before gel placement, k_w at S_{or} was 120 md in Berea, 4,000 to 6,500 md in polyethylene, and 140 to 640 md in fused silica. If $k_w = 0.26$ md at S_{or} after gel placement, F_{rrw} was 460 in Berea, 15,000 to 25,000 in polyethylene, and 540 to 2,400 in fused silica. Achieving a $(F_{rr} - 1)L_p$ parameter of 3,000 ft requires $L_p \geq 6.5$ ft in Berea. Smaller distances of gel penetration would be acceptable in the other porous media.

To summarize the significance of the previous calculations, consider a vertical production well with a two-wing vertical fracture that cuts through one oil zone and one water zone. Assume that both zones are Berea sandstone where $k_w = 120$ md at S_{or} and $k_o = 508$ md at S_{wr} before placement and $k_w = 0.26$ md at S_{or} and the ultimate $k_o = 100$ md at S_{wr} after placement of the Cr(III)-acetate-HPAM gel. This analysis suggested that the optimum distance of gel penetration from fracture faces should be at least 6.5 ft in the water zone but less than 10 ft in the oil zone. Of course, these distances apply only to this particular circumstance. The calculations must be repeated if the circumstances or input parameters are different.

Gel Penetration in Unfractured Wells. We advocate that hydrocarbon zones *must* be protected during gel placement in unfractured wells with radial flow (Liang et al. 1993; Seright 1988). However, upon observing the degree of cleanup during oil flow through gel (Figs. 1 and 7), we wondered whether exceptions might be found to our earlier beliefs. Close consideration of Fig. 14 indicates that for gel radii greater than 3 ft, oil residual resistance factors must be less than 2 to ensure minimum loss of oil productivity. This observation is consistent with our earlier findings (Liang et al. 1993; Seright 1988). Can F_{rr} values less than 2 be achieved reliably with the Cr(III)-acetate-HPAM gel? The discussion after Fig. 15 indicated that ultimate F_{rr} values might range from 1 to 5 in Berea, 2 to 5 in fused silica, and 5 to 76 in polyethylene. With the variations observed, it still seems unduly risky to inject gelant into unfractured wells without protecting the hydrocarbon zones from gel damage.

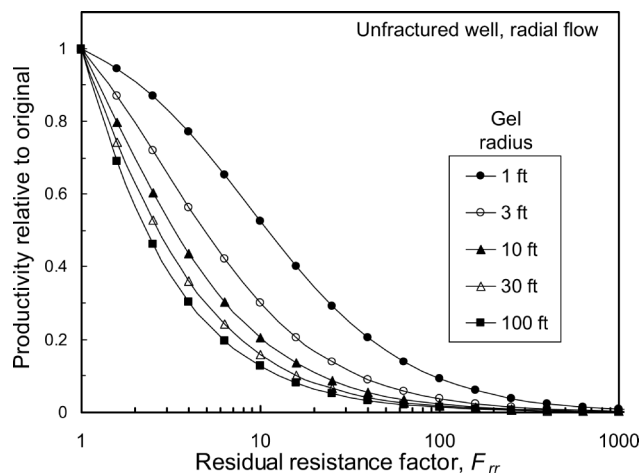


Fig. 14—Ultimate productivity after gel placement in an unfractured production well.

Behavior of an Adsorbed Polymer

The previously described work used a Cr(III)-acetate-HPAM gel that fills all aqueous pore space. Berea cores treated with an adsorbing polymer (i.e., solutions containing 0.18% BJ AquaCon™, 2% KCl) also exhibited permeabilities that increased gradually during the course of injecting 100 PV of oil (Seright 2002). In contrast to the Cr(III)-acetate-HPAM gel, this polymer did not occupy very much of the aqueous pore space and provided low water and oil residual resistance factors. Fig. 16 shows how permeability to oil increased with throughput for six experimental cases. In two cases (solid triangles and squares), oil was the first fluid injected after polymer placement. In these two cores, water was subsequently injected, followed by an additional cycle of oil (open triangles and squares). In two other cases (and separate cores), water was injected first after polymer placement, followed by oil injection (open circles and diamonds).

The thin and thick curves in Fig. 16 plot predictions from our model. The endpoint k_w and k_o input values used to generate the curves are indicated in Fig. 16. These curves did a reasonable job of bracketing the experimental data. However, the general shapes of the model curves did not follow the data trends as well as those for Cr(III)-acetate-HPAM gels (Fig. 7). The upper and lower curves were separated by a factor of seven in Fig. 7 and a factor of two in Fig. 16. As throughput increased from 1 to 100 PV, oil permeability increased typically by 5 to 10 in Fig. 7 and by 2 to 3 in Fig. 16.

Ultimate oil residual resistance factors (after 100 PV) ranged from 1.4 to 2.1 for the experiments in Fig. 16. On first consider-

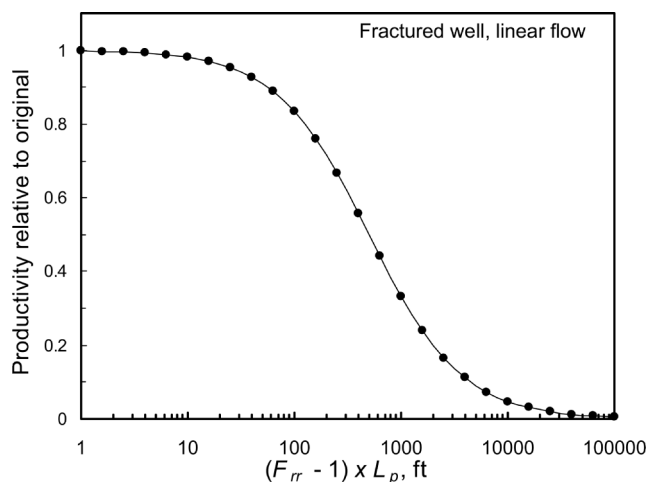


Fig. 15—Ultimate productivity after gel placement: linear flow, simplified correlation.

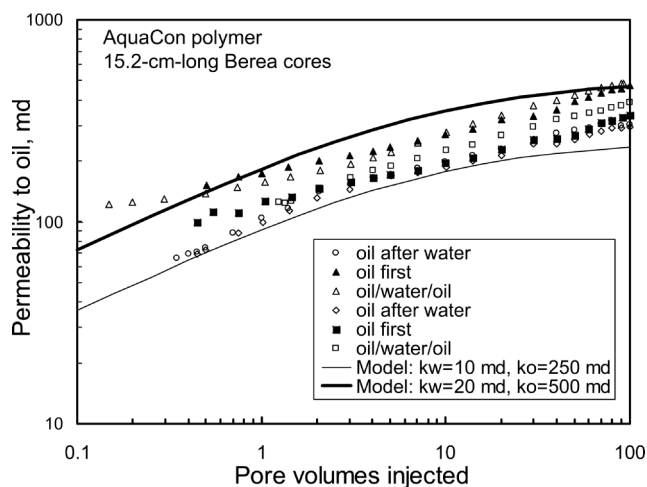


Fig. 16—Permeability during oil injection after treatment with an adsorbing polymer.

ation, these values might seem attractive for field applications—especially in unfractured wells (see Fig. 14). Unfortunately in these cases, water residual resistance factors were roughly the same as the oil residual resistance factors. (Water residual resistance factors and final permeability to water after polymer placement are listed in **Table 2**.) Consequently, within the variability of the experimental results, a polymer treatment would reduce productivities of oil and water zones by roughly the same factor.

In contrast to the behavior of the Cr(III)-acetate-HPAM gel, after treatment with the polymer, permeability to water often increased steadily over time (Seright 1988). This behavior could be caused by erosion or desorption of the polymer. Erosion or desorption of the polymer could also explain the difference between the model predictions and the oil experimental data in Fig. 16. At high throughput values, the model predicts that permeability to oil should level off, whereas the actual data continue to follow the same increasing trend—consistent with expectations for erosion or desorption.

In summary, after placement of an adsorbing polymer (AquaCon) in Berea, the permeability to oil increased significantly over the course of 100 PV. The polymer also provided fairly low oil residual resistance factors. Unfortunately, the polymer provided correspondingly low water residual resistance factors. If water residual resistance factors are too low, insufficient reduction in water productivity may be realized in field applications (Liang et al. 1993; Seright 1988; Seright website). For polymers and gels that provide similar residual resistance factors to oil and water, with values greater than two, hydrocarbon zones should be protected during gel placement (Liang et al. 1993; Seright 1988).

Note on Field Applications

In this paper, formation damage during a treatment was assumed to be caused by only gel or polymer. The application of a gel or polymer treatment was also assumed to not stimulate (increase)

hydrocarbon or water injectivity indexes. However, field cases have been reported [in the Arbuckle formation (Seright 2003)] in which gel treatments dramatically increased the oil productivity index. How could this happen? One possible explanation is as follows: When gelant or gel was injected into a production well, the downhole pressure was necessarily greater than at any time during production. If the well intersected fractures (either natural or artificially induced), the relatively high pressure during gel placement could force open the fracture or fracture system—thus stimulating the well and explaining why oil increased significantly. Why did the water productivity index not increase as well? Presumably, the explanation lies in the disproportionate permeability reduction provided by the gel. Opening the fracture system acted to stimulate both oil and water productivity, while gel in the matrix (of oil and water zones that were cut by the fracture) acted to diminish both oil and water productivity. The ultimate productivity index was determined by the relative importance of increased fracture area from pressurizing the well vs. the damage caused by the gel to the fracture areas in the oil and water zones. If the water residual resistance factor was sufficiently high, the water productivity index *decreased* even though the fracture area was increased during the treatment. If the oil residual resistance factor was sufficiently low, the oil productivity index *increased* even though the oil zone was damaged somewhat by the gel.

If the fracture area open to flow is changed by application of a polymer or gel treatment, that change must be quantified before predicting cleanup of oil productivity with our method.

Conclusions

The oil and water throughput requirements for stabilization of permeabilities were studied for a relatively “strong” pore-filling Cr(III)-acetate-HPAM gel and for a “weak” adsorbing polymer in cores. The following conclusions were reached:

1. As oil throughput increased from 1 to 100 PV, permeability to oil gradually increased by factors from 5 to 10 for cores treated with the Cr(III)-acetate-HPAM gel and from 2 to 3 for cores treated with the adsorbing polymer.
2. After treatment with Cr(III)-acetate-HPAM gel, permeability to water stabilized rapidly and remained stable for more than 6 months. In contrast, after treatment with the adsorbing polymer, permeability to water often increased steadily over time—possibly because of erosion or desorption of the polymer.
3. After placement of Cr(III)-acetate-HPAM gel in an 8-darcy polyethylene core, the minimum pressure gradient to initiate oil flow was between 1.3 and 1.7 psi/ft.
4. A simple mobility-ratio model predicted cleanup times for both fractured and unfractured wells after a gel treatment. The time to restore productivity to a gel-treated oil zone
 - Was similar for radial vs. linear flow.
 - Varied approximately with the cube of distance of gel penetration.
 - Varied inversely with pressure drawdown.
 - Varied inversely with k_w at S_{or} in the gel-treated region.
 - Was not sensitive to the final k_o at S_{wr} .
5. Although k_o at S_{wr} (after gel placement) had no effect on the cleanup time, it strongly affected how much of the original oil productivity could ultimately be regained.

TABLE 2— k_w VALUES AFTER POLYMER PLACEMENT IN BEREA

Condition	Initial Core (k , md)	k_w at S_{or} (before gel) (md)	k_w at S_{or} (after gel) (md)	F_{rw}
Water 1st	498	126	64.3	2.0
2nd water after oil	498	126	38	3.3
Water after oil	853	293	93.3	3.1
Water 1st	469	124	84.4	1.5
2nd water after oil	469	124	95.5	1.3
Water after oil	913	310	52.2	5.9

6. Consistent with earlier work, the new results and analysis confirmed that in radial matrix flow (e.g., unfractured wells), hydrocarbon productive zones *must* be protected during gelant or polymer placement.

Nomenclature

F_{rr} = residual resistance factor (mobility before gel divided by mobility after gel)
 F_{rro} = oil residual resistance factor
 F_{rrw} = water residual resistance factor
 k = permeability, md [μm^2]
 k_o = permeability to oil, md [μm^2]
 k_{ro} = relative permeability to oil
 k_{ro}^o = relative permeability to oil at S_{wr}
 k_{rw} = relative permeability to water
 k_{rw}^o = relative permeability to water at S_{or}
 k_w = permeability to water, md [μm^2]
 k/μ = mobility, md/cp [$\mu\text{m}^2/\text{mPa}\cdot\text{s}$]
 $(k/\mu)_o$ = oil mobility, md/cp [$\mu\text{m}^2/\text{mPa}\cdot\text{s}$]
 $(k/\mu)_w$ = water mobility, md/cp [$\mu\text{m}^2/\text{mPa}\cdot\text{s}$]
 L_e = external drainage distance, ft [m]
 L_p = distance of gelant penetration, ft [m]
 M = mobility ratio
 no = oil saturation exponent in Eq. 4
 nw = water saturation exponent in Eq. 3
 Δp = pressure drop, psi [Pa]
 q = injection or production rate after gel placement, B/D
 q_{final} = ultimate oil production rate after gel, B/D [m^3/d]
 q_o = injection or production rate before gel, B/D [m^3/d]
 r_e = external drainage radius, ft [m]
 r_p = radius of gelant penetration, ft [m]
 r_w = wellbore radius, ft [m]
 S_{or} = residual oil saturation
 S_w = water saturation
 S_{wr} = residual water saturation
 t = time, d

Acknowledgments

Financial support for this work is gratefully acknowledged from the United States Department of Energy (NETL/National Petroleum Technology Office), the State of New Mexico, ConocoPhillips, ExxonMobil, and Marathon. John Hagstrom and Richard Schrader conducted the experiments. I thank Julie Ruff and Robert Sydansk for reviewing this paper.

References

- <http://baervan.nmt.edu/andy/>
 Koval, E.J. 1963. A Method for Predicting the Performance of Unstable Miscible Displacement in Heterogeneous Media. *SPEJ* 3(3):145–154; *Trans.*, AIME, 228.
 Krishnan, P., Asghari, K., Willhite, G.P., McCool, C.S., Green, D.W., and Vossoughi, S. 2000. Dehydration and Permeability of Gels Used in In-Situ Permeability Modification Treatments. Paper SPE 59347 presented at the SPE/DOE Improved Oil Recovery Symposium, Tulsa, 3–5 April.
 Lake, L.W. 1989. *Enhanced Oil Recovery*. Englewood Cliffs, NJ: Prentice-Hall. 61.
 Lane, R.H. and Sanders, G.S. 1995. Water Shutoff Through Full-Bore Placement of Polymer Gel in Faulted and in Hydraulically Fractured

Producers of the Prudhoe Bay Field. Paper SPE 29475 presented at the SPE Production Operations Symposium, Oklahoma City, Oklahoma, 2–4 April.

- Liang, J., Lee, R.L., and Seright, R.S. 1993. Gel Placement in Production Wells. *SPEPF* 8(4):276–284; *Trans.*, AIME, 295. SPE-20211-PA.
 Marin, A., Seright, R., Hernandez, M., Espinoza, M., and Mejias, F. 2002. Connecting Laboratory and Field Results for Gelant Treatments in Naturally Fractured Production Wells. Paper SPE 77411 presented at the SPE Annual Technical Conference and Exhibition, San Antonio, Texas, 29 September–2 October.
 Seright, R.S. 1988. Placement of Gels To Modify Injection Profiles. Paper SPE/DOE 17332 presented at the SPE/DOE Enhanced Oil Recovery Symposium, Tulsa, 16–21 April.
 Seright, R.S. 1991. Impact of Dispersion on Gel Placement for Profile Control. *SPEE* 6(3):343–352. SPE-20127-PA.
 Seright, R.S. 1993. Effect of Rock Permeability on Gel Performance in Fluid-Diversion Applications. *In Situ* 17(4):363–386.
 Seright, R.S. 2002. Conformance Improvement Using Gels. Annual Technical Progress Report (U.S. DOE Report DOE/BC/15316-2), U.S. DOE Contract DE-FC26-01BC15316, 43–59.
 Seright, R.S. 2003. Conformance Improvement Using Gels. Annual Technical Progress Report (U.S. DOE Report DOE/BC/15316-4), U.S. DOE Contract DE-FC26-01BC15316, 39–45.
 Seright, R.S. 2004. Conformance Improvement Using Gels. Annual Technical Progress Report (U.S. DOE Report DOE/BC/15316-6), U.S. DOE Contract DE-FC26-01BC15316, 82–87.
 Seright, R.S. 2006. Optimizing Disproportionate Permeability Reduction. Paper SPE 99443 presented at the SPE/DOE Symposium on Improved Oil Recovery, Tulsa, 22–26 April.
 Seright, R.S., Liang, J., and Seldal, M. 1998. Sizing Gelant Treatments in Hydraulically Fractured Production Wells. *SPEPF* 13(4):223–229. SPE-52398-PA.
 Seright, R.S., Prodanovic, M., and Lindquist, W.B. 2006. X-Ray Computed Microtomography Studies of Disproportionate Permeability Reduction. *SPEJ* 11(2) (in process).
 Stanley, F.O., Hardiatio, E., and Tanggu, P.S. 1996. Improving Hydrocarbon/Water Ratios in Producing Wells—An Indonesian Case History Study. Paper SPE 36615 presented at the SPE Annual Technical Conference and Exhibition, Denver, 6–9 October.
 Zaitoun A. and Kohler, N. 1988. Two-Phase Flow Through Porous Media: Effect of an Adsorbed Polymer Layer. Paper SPE 18085 presented at the SPE Annual Technical Conference and Exhibition, Houston, 2–5 October.

SI Metric Conversion Factors

cp × 1.0*	E-03 = Pa·s
ft × 3.048*	E-01 = m
in. × 2.54*	E+00 = cm
md × 9.869 233	E-04 = μm^2
psi × 6.894 757	E+00 = kPa

*Conversion factors are exact.

Randy Seright is a senior engineer at the New Mexico Petroleum Recovery Research Center at New Mexico Tech in Socorro. E-mail: randy@prrc.nmt.edu. He was an SPE Distinguished Lecturer for 1993–1994 and holds a PhD degree in chemical engineering from the U. of Wisconsin at Madison.